A Holistic Work Zone Safety Alert System through Automated Video and Smartphone Sensor Data Analysis

December 2022 | Final Report

SAFE-D
SAFETY THROUGH DISRUPTION

Texas A&M Transportation Institute

San Diego State University
Leadership Starts Here

VIRGINIA TECH TRANSPORTATION INSTITUTE
VIRGINIA TECH

Disclaimer

The contents of this report reflect the views of the authors, who are responsible for the facts and the accuracy of the information presented herein. This document is disseminated in the interest of information exchange. The report is funded, partially or entirely, by a grant from the U.S. Department of Transportation's University Transportation Centers Program. However, the U.S. Government assumes no liability for the contents or use thereof.

TECHNICAL REPORT DOCUMENTATION PAGE

1. Report No. 05-089	2. Government Accession No.	3. Recipient's Catalog No.
4. Title and Subtitle A Holistic Work Zone Safety Alert System through Automated Video and Smartphone Sensor Data Analysis		5. Report Date 12/16/2022 6. Performing Organization Code:
7. Author(s) Reza Akhavian (SDSU) Arash Jahangiri (SDSU) Farid Shahnavaz (SDSU) Sina Salehipour (SDSU)		8. Performing Organization Report No. 05-089
9. Performing Organization Name and Address: Safe-D National UTC San Diego State University		10. Work Unit No. 11. Contract or Grant No. 69A3551747115/Project 05-089
12. Sponsoring Agency Name and Address Office of the Secretary of Transportation (OST) U.S. Department of Transportation (US DOT)		13. Type of Report and Period Final Research Report Start Date: 1/11/20 End Date:12/16/22 14. Sponsoring Agency Code

15. Supplementary Notes
This project was funded by the Safety through Disruption (Safe-D) National University Transportation Center, a grant from the U.S. Department of Transportation – Office of the Assistant Secretary for Research and Technology, University Transportation Centers Program.

16. Abstract
This project was inspired by a major gap identified in the literature pertaining to work zone safety monitoring systems that leverage advanced technologies for tracking workers, identifying hazardous situations, and alerting workers of danger. Existing systems target safety hazards that are either external to the work zone (e.g., accidents due to vehicular intrusions) or workers' internal physical/physiological states (e.g., human-factor ergonomics such as improper or prolonged use of vibrating hand tools). This project presents a holistic approach in which visual and wearable sensor data are used for safety monitoring and alert generation to offer a practical mitigation strategy to both external and internal safety risks. With a major focus on feasibility of adoption and facilitating maintenance, smartphones were used in this project to provide a ubiquitous platform for data collection and communication. A mobile application was developed to generate an alert when unsafe vibration levels were reached in proximity to a high vibration power tool such as a jackhammer. Additionally, visual data collected from surveillance cameras were analyzed to detect speeding vehicles approaching the work zone. In either of these situations, a worker with the application running on their smartphone would be alerted of the internal or external safety hazard.

17. Key Words Publication, guidelines, report, brochure, communication, marketing	18. Distribution Statement No restrictions. This document is available to the public through the Safe-D National UTC website, as well as the following repositories: VTechWorks, The National Transportation Library, The Transportation Library, Volpe National Transportation Systems Center, Federal Highway Administration Research Library, and the National Technical Reports Library.

19. Security Classif. (of this report) Unclassified	20. Security Classif. (of this page) Unclassified	21. No. of Pages 20	22. Price $0

Form DOT F 1700.7 (8-72) Reproduction of completed page authorized

Abstract

This project was inspired by a major gap identified in the literature pertaining to work zone safety monitoring systems that leverage advanced technologies for tracking workers, identifying hazardous situations, and alerting workers of danger. Existing systems target safety hazards that are either external to the work zone (e.g., accidents due to vehicular intrusions) or workers' internal physical/physiological states (e.g., human-factor ergonomics such as improper or prolonged use of vibrating hand tools). This project presents a holistic approach in which visual and wearable sensor data are used for safety monitoring and alert generation to offer a practical mitigation strategy to both external and internal safety risks. With a major focus on feasibility of adoption and facilitating maintenance, smartphones were used in this project to provide a ubiquitous platform for data collection and communication. A mobile application was developed to generate an alert when unsafe vibration levels were reached in proximity to a high vibration power tool such as a jackhammer. Additionally, visual data collected from surveillance cameras were analyzed to detect speeding vehicles approaching the work zone. In either of these situations, a worker with the application running on their smartphone would be alerted of the internal or external safety hazard.

Acknowledgements

This project was funded by the Safety through Disruption (Safe-D) National University Transportation Center, a grant from the U.S. Department of Transportation – Office of the Assistant Secretary for Research and Technology, University Transportation Centers Program. The research team would like to acknowledge the support from Casper Company for granting access to their job site for data collection. We would also like to thank Dr. Christopher Paolini and Dr. Ashkan Ashrafi at SDSU for their expert consultation as well as SDSU student volunteers, Amir Mohammad Moradi, Django Bergcollins, and Siamak Doraghi. We also appreciate the support and feedback provided by the project's subject matter expert, Dr. Nazila Roofigari-Esfahan.

Table of Contents

List of Figures

List of Tables

Introduction

Due to growing highway reconstruction needs, future construction work zones are likely to expand in number, exist over greater project durations, and be larger in terms of the amount of work needed. The Federal Highway Administration and the American Traffic Safety Service Association have raised concerns about the safety of workers in the construction industry due to the high rate of serious injuries and accidents in work zones (Baron, 2004; Nnaji et al., 2020). Each year there are more than 700 deaths and 44,000 injuries in work zones in the United States; in 2020, the number of work zone accidents in the U.S. reached 31,000 (National Work Zone Data, 2022).

Work zone construction workers are exposed to both internal and external safety risks. Internal risks refer to potential injuries as a result of ergonomic hazards, whereas external risks concern the possibility of accidents with oncoming vehicles. Injuries due to improper or prolonged use of hand tools are examples of internal or ergonomic risks and motor vehicles speeding towards or near work zones illustrate possible external risks. While overexertion and awkward postures are usually the focus of ergonomic analysis of the fieldworkers' activities, vibration is another, less-studied, etiologic cause of certain injuries such as chronic nerve and tendon disorders (Armstrong et al., 1987).

Most of the power tools and hand equipment used by fieldworkers in industries such as construction produce some level of vibration. Road and infrastructure construction work zones, for example, often involve power tools that are required to cut or break large concrete or asphalt segments. Those devices help workers perform construction tasks that are too physically demanding to be carried out manually. However, if used frequently and continuously without appropriate break times, such devices can pose bodily injury threats to workers. The most common resulting injury in such situations is hand-arm vibration syndrome (HAVS), where the delicate nerve and muscle tissues of the hands and fingers are damaged by strong vibrations (Savage et al., 1990; Ho & Yu, 1989). Work zone workers who use vibrating equipment (e.g., power drills, handsaws, jackhammers, pneumatic drills) more frequently as part of their job are more likely to damage their hand and arm nerves. Vibrations can impair blood flow to the fingers, which in turn can lead to loss of sensation and impaired hand functions. Numbness, pain, and blotchiness are some of the signs and symptoms of such injuries (Lundborg et al., 1987; Miller et al., 1994; Takeuchi et al., 1988). Studies have shown that 2.5 million workers in the U.S. are potentially exposed to HAVS (Alvarez, Bogen, & Levine, 2019). The National Institute for Occupational Safety and Health has emphasized the seriousness of vibration syndrome, and recommend that workers, employers, and occupational health professionals implement engineering controls, medical surveillance, and work practices along with personal protective equipment to mitigate associated risks (Bernard et al., 1998). An analysis of the neurosensory components of HAVS was conducted over a 22-year period to determine the syndrome's progression and prognostic factors. The results indicated that hand numbness and finger pain in workers with HAVS are not

completely reversible and continued exposure to vibration results in growing pain in fingers (Aarhus et al., 2019). Given the evidence presented in the previous studies, it can be concluded that while standards are imperative to mitigate HAVS, a practical approach towards ensuring that the standard are in fact adopted in the design of work shifts and breaks to limit the exposure to vibration is an important supplementary approach.

In addition to safety issues concerning power tools vibrations, vehicular intrusions into work zones also threaten workers' safety and lives. Speeding has been identified as one of the most important factors that could cause crashes on the roadways, particularly in active work zones, where there is a higher chance of crash occurrence since road users need to drive slower than usual and be more attentive around these areas. To reduce the chance of crashes, more proactive methods of safety assessment are required, ideally in real-time. Existing condition analysis must be made first, to provide the foundation of accident prevention design. Such analysis includes detecting and monitoring the speed of the vehicles within the investigated area. Current speed detection methods may use LIDAR, but not all vehicles and infrastructure are equipped with this or other related technologies. Existing surveillance cameras in cities, which are ubiquitous in many locations nowadays could potentially be used to monitor speeding events. In the last several decades, artificial intelligence and particularly computer vision techniques that leverage the data collected by these cameras, have excelled in resolving a wide range of real-world traffic applications.

Informed by the statistics of workers' safety issues in work zones and inspired by recent advancements in pervasive sensing devices and computing powers, this project aimed at developing a holistic approach to recognize a hazard and inform workers to respond in time. The assumption is that a framework that can detect safety risks and warn work zone workers in real-time could help mitigate the risk of potential injuries. Toward this goal, a smartphone application was developed to detect internal and external risks (as defined above) and alert exposed workers. This is an integrated system that captures signals from the smartphone sensors as well as cameras installed on the road leading to the work zone. The system then analyzes the data on a server to detect potential hazards and send alerts. More specifically, whenever there is a safety risk, such as a worker exposed to excessive vibration or to a vehicle speeding toward the work zone, the smartphone application informs the worker by generating alerts. This research leverages live video feed from an intersection in the City of Chula Vista. CA to detect and monitor vehicles' speed and generate warning messages when speed goes above a certain threshold. Subsequently, the messages are sent to workers to increase their awareness of the impending danger. Figure 1 shows the schematic overview of the developed framework.

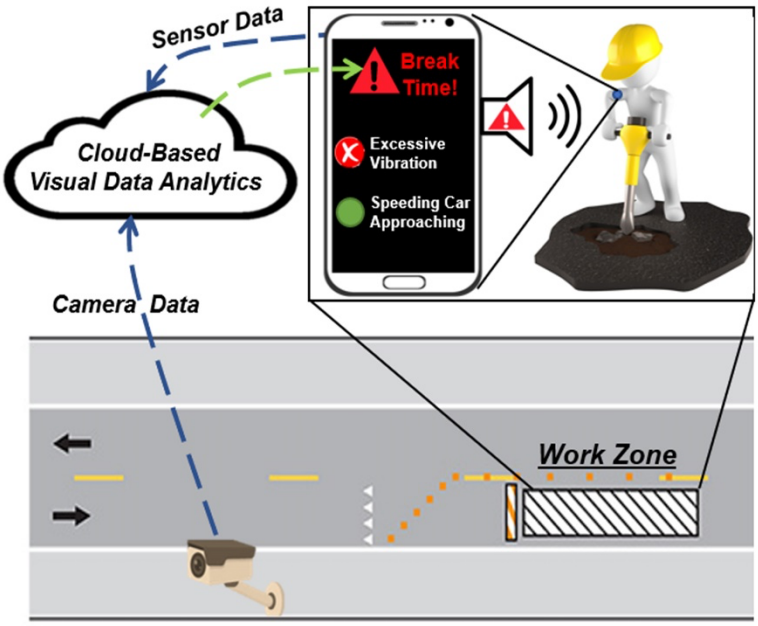

Figure 1. Schematic overview of the developed framework.

Monitoring Workers' Hand-Arm Vibration Levels

Hand-Arm Vibration Safety in Industrial Applications Background

In general, there are two main types of vibratory effects on the human body: hand-arm vibration (HAV) and whole-body vibration (WBV; Coggins et al., 2010). HAV refers to when the hand grips vibrating equipment or tools such as power drills, handsaws, jackhammers, and pneumatic drills. WBV, on the other hand, pertains to using a vibrating surface to support the body; for example, a vibration platform would allow one to exercise in a variety of static positions (Coggins et al., 2010).

Several previous studies have investigated HAV. Shen and House (2017) introduced HAVS as a negative consequence of using hand-held vibrating tools for a long time. Three components make up the syndrome: vascular, represented by the secondary Raynaud phenomenon (Griffin & Bovenzi, 2002); sensorineural; and musculoskeletal. In its more advanced stages, HAVS is associated with significant disability and poor quality of life (Pelmear & Leong, 2000). When diagnosed with HAVS, vibration exposure should be reduced, cold conditions should be avoided, smoking should be stopped, and medication should be administered (Shen & House, 2017).

As for WBV, Bovenzi et al. (2017) studied three groups of professional drivers for the risks of occupational vibration injuries as part of a 4-year research project. These drivers operated equipment such as earth-moving machines, fork-lift trucks, and public utilities vehicles. The result showed that A(8) (i.e., the daily vibration exposure value normalized to an eight-hour reference period, explained in detail later) and VDV (i.e., the Vibration Dose Value) are significantly greater

than A(8)max and VDVmax, which are the maximum safe values as prescribed in the international standard ISO 2631-1, which is dedicated to the effects of WBV on health (International Standards Organization [ISO], 1997). Researchers have also considered this as evidence of the associations between low back disorders and occupational exposures to WBV (Bovenzi et al., 2017). Other studies, including a comprehensive review of WBV injuries in 2015 have also concluded that there are strong associations between WBV exposure and low back pain or sciatica (Burnström et al., 2015). The risk of unsafe levels of WBV on construction workers has also been explored. For example, a group of scholars at the University of Granada implemented an assessment of WBV using two standards: ISO 2631-1:2008 and ISO2631-5:2018. One of the study's main conclusions was that the surface roughness level is a crucial factor related to WBV in construction workers and especially heavy equipment drivers (Hoz Torres et al., 2019).

Sensor-based Fieldworker Safety Monitoring Background

The findings of the studies reviewed above have resulted in valuable standards and guidelines indicating that unsafe levels of vibration and repetition have serious safety and health effects on workers. Nevertheless, unobtrusive monitoring of such hazardous exposures in construction workers with the goal of preventing injuries has received very little attention in the literature. Construction workers' safety has been improved by developing practical and unobtrusive solutions that collect and classify construction activities. With wearable sensors and video cameras, researchers have developed data-driven simulation models with safety and productivity monitoring applications (Akhavian & Behzadan, 2016; Jeelani et al., 2021; Kim & Cho, 2021). For example, Akhavian and Behzadan (2016) used smartphone-based wearable sensors for workers' safety monitoring in construction activities, although no established safety or health standard was used to determine the level of hazards, and in particular vibration hazards, imposed on the workers. Aryal et al., (2016) used heart rate monitors, infrared temperature sensors, and an EEG (i.e., electroencephalogram) sensor for monitoring fatigue in construction workers. However, their work was limited to applying a specific health standard to create a response system for laborers (Aryal, et al., 2017). In another study, Cheng et al. (2013) used a Physiological Status Monitoring system that included a wearable electrocardiograph (ECG) sensor, a respiration sensor, and a three-axial accelerometer to monitor physiological status during construction work (Cheng et al., 2013). Smartphone app-based systems that leverage embedded sensors have been also developed and used for tracking construction workers' movements in an unobtrusive manner, enabling safety and ergonomic monitoring and tracking (Jahanbanifar & Akhavian, 2018; Yang et al., 2019).

While there are numerous past studies that leverage the safety standards with regards to vibration analysis as well as those that monitor safety using wearable sensors, these two approaches have never been investigated in conjunction with each other for construction workers' safety. The presented study aims to fill this gap in the body of knowledge by introducing smartphone-based vibration data collection and threshold analysis for construction workers that considers the nature of the work in common road work zone operations.

Hand-Arm Vibration Safety Standards

To mitigate the negative effects of prolonged exposure to HAV, safety training procedures and standardization content have been developed by different health organizations. For example, the World Health Organization suggests using the ISO 5349-1:2001 standard, which takes into account the measurement and evaluation of human exposure to hand-transmitted vibration (ISO, 2001). The Threshold Limit Values standard, presented at the American Conference of Governmental Industrial Hygienists, is another measure for WBV (Castleman & Ziem, 1994). Examples from outside the United States include work by the Japan Society for Occupational Health, which developed the Occupational Exposure Limits standard to deal with adverse health effects on workers caused by WBV, HAV, or chemical substances (Omae et al., 1999).

Different local or international standards set limitations for the amount of vibration that workers can be exposed to without posing any safety and health issues (M. Griffin, 1980; Langsley et al., 1981). ISO/DIS 5349:1986 is one of the most important standards proposed with regards to HAV. Hand-transmitted vibration exposure is measured and reported according to a draft standard that explains how these measurements are related to limited epidemiological data (ISO, 1986). While this is the latest ISO standard on this subject, and serves as a valuable safety measurement benchmark, it is not completely practical in use since vibration is often difficult to measure and there is no quantitative relationship between vibration levels and health effects. The American National Standards Institute (ANSI) uses the same method introduced by ISO to set a threshold for the level of vibration (ANSI, 2006). The method is described below.

According to ISO/DIS 5349: 1986, vibrations are described by the root-mean-square acceleration (*rms*), in meters per second squared (m/s2). Equation (1) is used to calculate *rms* single axis ISO frequency-weighted acceleration value.

$$a_{hw(rms)} = \sqrt{\frac{1}{T}\int_0^T a_{hw}^2(t)dt} \qquad (1)$$

where $a_{hw}(t)$ is the instantaneous single axis ISO frequency-weighted acceleration value as a function of time, and t is the integration time in seconds (s).

Frequency bands (i.e., intervals in the frequency domain) are used to extract useful levels of signal with acceptable distortion characteristics needed for a specific application (ANSI, 2006). An octave band is a frequency band that spans one octave. In the one-third octave band where frequency ranges between 6.3 and 1,250 Hz, the single-axis acceleration values may be specified as one-third octave band values. Equation (2) gives the values of ahi(rms) for one-third octave band *rms* single-axis acceleration.

$$a_{hi(rms)} = \sqrt{\frac{1}{T}\int_0^T a_{hi}^2(t)dt} \qquad (2)$$

where *ahi(t)* is the instantaneous single-axis one-third octave band acceleration value as a function of time in the i^{th} one-third octave frequency band, and *T* is the integration time in seconds (s).

By summarizing the one-third octave band *rms* single-axis acceleration values from 6.3 to 1,250 Hz, the *rms* single-axis ISO frequency-weighted acceleration value, *ahw(rms)*, can be developed using Equation 3.

$$a_{hw(rms)} = \sqrt{\sum_i (W \ a_{hi(rms)})^2} \quad (3)$$

where W_{hi} is the ISO frequency-weighting factor for the i^{th} one-third octave frequency band. The table of the W_{hi} is represented in Appendix A. For vibration measurements using a smartphone accelerometer, the coordinate system should be defined in reference to the smartphone coordinate system (see Figure 2). The orientation of the coordinate system used for measurement must be reported with respect to distances and angles from the coordinate system.

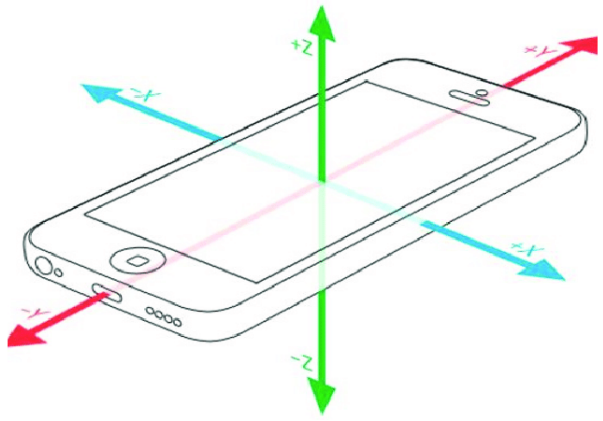

Figure 2. The coordinate system for the smartphone.

For a single operation that involves hand-transmitted vibration exposure, the vibration total value, $ahv_{(rms)}$, is determined by the root-sum-squares of the measured *rms* ISO frequency-weighted acceleration values in the x, y, and z directions, as shown in Figure 2. For the vibration total value, $ahv_{(rms)}$, the variable is a characteristic of the hand-arm system according to ISO 5349. It is calculated by Equation 4.

$$a_{hv(rms)} = \sqrt{a_{hwx(rms)}^2 + a_{hwy(rms)}^2 + a_{hwz(rms)}^2} \quad (4)$$

An acceleration magnitude in the x, y, and z directions is measured as a function of ISO frequency-weighted acceleration magnitudes *ahwx(rms), ahwy(rms), and ahwz(rms)*, respectively.

Assuming that the vibration total value, *ahv(rms)*, associated with the hand-transmitted vibration exposure of a worker is composed of several operations, each with a different vibration magnitude, then the vibration total value should be calculated using Equation (5).

$$a_{hv(rms)} = \sqrt{\frac{1}{T_v}\sum_{i=1}^{n}(a_{hv(rms)i}^2 T_i)} \quad (5)$$

The vibration total value $a_{hv(rms)i}$ is the vibration total value associated with the i^{th} operation, *Ti* is the time duration in hours associated with the i^{th} operation, n is the total number of operations, and *Tv* is the total amount of time associated with the n operations.

From Equation (6), the vibration exposure value, *A(8)*, can be obtained and is standardized to an 8-hour reference period:

$$A(8) = a_{hv(rms)}\sqrt{\frac{T_v}{T_0}} \quad (6)$$

T_0 is the reference duration of 8 hours. The vibration exposure *A(8)* represents a worker's daily exposure to vibration.

According to the ANSI standard, the Daily Exposure Action Value (DEAV) is 2.5 m/s^2 (ANSI, 2006). This value can be used to determine the health risk threshold for hand-transmitted vibration. As defined in this standard, the health risk threshold is the level of hand-transmitted vibration exposure that is sufficient to cause abnormal signs, symptoms, and laboratory findings in the vascular, bone or joint, neurological, or muscular systems of the hands and arms in some exposed individuals (Reynolds, 2006). ANSI also prescribes the Daily Exposure Limit Value (DELV) of 5.0 m/s^2 (ANSI, 2006). Vibrations transmitted by the hand at or above this level are expected to pose a high health risk to workers. The difference between DEAV and DELV is on the intensity level acceptable for a given task. While DEAV should be avoided, DELV is the ultimate level that must not be reached under any circumstances considering the health effects. Therefore, DEAV is used in this research as a threshold for the purpose of alerting workers at risk.

Considering a case where T_v is not the standard 8-hour exposure time, the vibration total value, $a_{hv(rms)}$, can be represented as follows:

$$a_{hv(rms)} = \sqrt{\frac{8}{T_0}}.A(8) \quad (7)$$

For an exposure time other than 8 hours that has a vibration total, $a_{hv(DEAV)}$, these values are calculated as follows:

$$a_{hv(DEAV)} = 2.5\sqrt{\frac{8}{T_v}} \quad (8)$$

Thus, the T_v, the duration that the worker can perform a task at a constant level without a potential safety risk, is calculated using Equation 9.

$$T = \frac{50}{a^2_{hv(DELV)}} \quad (9)$$

Method

The developed framework consists of a smartphone (i.e., embedded sensors, an application with a graphical user interface [GUI], and data transmission), software codes responsible for managing the process and calculating the results and a server to make a connection between them. The smartphone accelerometer sensors measure 3D acceleration of the body part where it is located and use the GUI to communicate the collected data and alarm values, when A(8) exceeds the threshold. The smartphone application was developed using Flutter framework and the Dart programming language in the front-end, and the software codes were programmed in Python language on the back-end. The back-end is responsible for collecting data, signal processing, calculation, and determining if the threshold has exceeded. The front-end is the interface of the application and shows the vibration exposure timer and acceleration speed of oncoming vehicles. Flask, a web development framework in Python programming language (Grinberg, 2018), was used to establish the connection between the system's back-end and front-end (Wijethunga & Ilmini, 2020). Figure 3 shows the framework of the system.

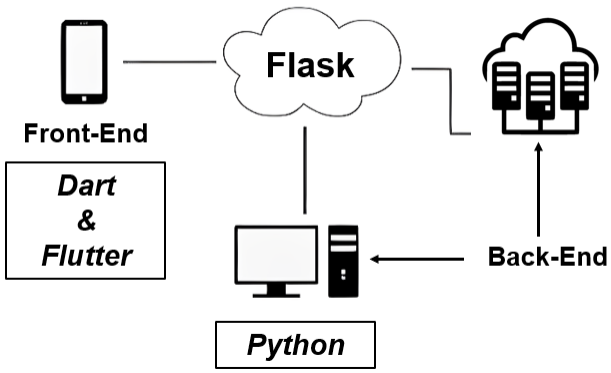

Figure 3. Data management and analysis framework.

Vibration Data Collection

In order to ensure high-fidelity data collection, the process of collecting data was conducted in an uncontrolled environment in which the workers were engaged in their everyday routines without interruption from researchers. A built-in smartphone accelerometer was used to collect the vibration data from a worker who was operating a jackhammer. A phone was attached to both of

the worker's arms to ensure redundancy in data collection. The accelerometer data in the form of $a_{hix(rms)}$, $a_{hiy(rms)}$, and $a_{hiz(rms)}$, was stored in the server. The sampling frequency was set at 500 Hz. Figure 4 shows the worker with smartphones attached to both arms. The developed application is installed on both smartphones and data is collected using both. An initial screening of the data collected showed a consistently similar timeseries data in the datasets generated by both data collection nodes and one of them (i.e., the one installed on the right hand arm) was used as the data source.

Figure 4. Smartphones worn by the worker on both arms.

The worker who wore the smartphones used two power tools: a Hilti TE 1000 AVR and a Makita HM1203C. Figure 5 illustrates the equipment used and Table 1 shows the tool specifications, including the model, weight, impact energy and blows per minute. At the time of data collection, a research team member was monitoring the data collection on the server and another team member was video recording the entire data collection for later cross-check and analysis (Figure 6). There were a total of three workers on the job site. One of them was using a jackhammer for floor demolition and the other two were helping with watering the area and cleaning the surface (**Error! Reference source not found.**).

Figure 5. Two different jackhammer types were used by the worker.

Table 1. Jackhammer Specifications

Jackhammer	Model	Weight (lbs.)	Impact Energy (ft-lbs.)	Blows Per Minute (variable speed)
1	TE 1000 AVR	27.7	19.2	1950
2	HM1203C	20.3	18.8	950-1900

Figure 6. A) The worker using the TE 100 AVR, B) The worker using the HM1203C, C) The data collection scene with research team members.

Signal Processing for Safety Standard Evaluations

Imported data was processed according to the standards then important features were extracted. By dissecting the signal into different frequency ranges and measuring the *rms* acceleration value for each of those ranges, a Fourier spectrum analyzer can determine the frequency spectrum of acceleration. First $a_{hwx(rms)}$, $a_{hwy(rms)}$, *and* $a_{hwz(rms)}$ were calculated according to the analysis, provided an *rms* acceleration value for each 1/3-octave center band frequency from 6.3 to 1250 Hz, for each of the three axes using Equation 3. Then $a_{hv(rms)}$ was obtained by the root-sum-squares of the measured *rms* (Equation 4) Rather than taking into account the time intervals between measurements, this was the average exposure for the events measured from the worker.

Smartphone Application GUI

Figure 7 illustrates the application's GUI. The interface shows the value of acceleration in each direction at each point in time. The *Timer* that expresses the remaining duration of time at the current level of vibration to adhere to safety standards. The risk level indicates if the current situation is unsafe (i.e., past the DEAV) or not. If the level rises past the DEAV, the *Risk Level* changes to *STOP WORK*, indicating that the worker should stop the work for the day. Buttons are also available to *Start*, *Stop*, or *Restart* the process. The *Check Cars* button starts the process of monitoring approaching cars automatically. When the user presses the start button, the timer starts working. The user can stop the timer or restart it if a new worker wants to continue the job. By pressing the C*heck Cars* button, the application starts listening to the server for any signal which received indicating that a speeding vehicle is approaching the work zone.

To calculate the remaining time for the worker to continue the work using the vibratory tool at a safe level, the application essentially calculates $a_{hv(rms)}$ in the signal processing component. The remaining allowed duration of work is calculated by Equation 9 and presented here. The application is dynamic in calculating this duration. More specifically, it considers the fact that the worker may not work non-stop on the given task that involves the high vibratory power tool and may engage in other tasks or take a break. As such, the timer is updated as the program stores the $a_{hv(rms)}$ cumulatively and re-computes the T_v every minute. If the worker does not stop working and continues the task without a break or switches to another task with a level of vibration, the timer eventually shows zero, which is when an alarm is triggered and warns the worker to stop. In other words, when the alarm goes off, it means that the cumulative DEAV has reached 2.5 m/s^2. The warning is a combination of an auditory and vibratory alarm.

Figure 7. GUI of the developed application.

Hazardous Vibration Detection Results and Discussion

Table 2 provides the $a_{hv(rms)}$ values of each event based on the tasks that the worker performed. The worker started with breaking a concrete slab for 1 hour using the *TE 1000 AVR* equipment (shown in **Error! Reference source not found.**). After a 15-minute break, the worker continued the same task for 25 minutes. Then the worker switched to using the *HM1203C* jackhammer (see **Error! Reference source not found.**) and worked on the same task for another 18 minutes before the alarm on the developed application went off.

Table 2. Event Logs

Activity	Tool	Duration (minutes)	$a_{hv(rms)}$ (m/s^2)
Break Concrete Slab	TE 1000 AVR	58	5.99
Rest	-	15	0
Break Concrete Slab	TE 1000 AVR	25	5.99
Switching Tool	-	1	0
Break Concrete Slab	HM1203C	18	0.98

For each event, weighted acceleration ($a_{hv(rms)}$) values were calculated using Equation (4). $a_{hv(rms)}$ values were calculated for each axis and the largest $a_{hv(rms)}$ of the three axes was chosen as the $a_{hv(rms)}$ for the event and represented in the last column. Time-remaining (T_v) in each moment was calculated using Equation (9). To estimate the worker's exposure levels throughout a full shift, the tool operation time should be divided by the total duration of work, including periods between measurements, and the value multiplied by 8 hours. Then the vibration total value can be obtained using Equation (5):

$$a_{hv(rms)} = \sqrt{\frac{1}{101}(5.99^2 \times 58 + 5.99^2 \times 25 + 0.98^2 \times 18)} = 5.45$$

where 101 is the total time in minutes associated with the operation of the equipment. Finally, *A(8)* can be calculated for this worker using Equation (6). Assuming a work shift was 8 hours (i.e., equal to 480 minutes):

$$A(8) = 5.45\sqrt{\frac{101}{480}} = 2.5$$

The *A(8)* of 2.5 m/s^2 indicates that the alarm went off at the correct point in time where the threshold of DEAV was reached. As such, the research team asked the worker to stop and take a break.

Detection of Cars Speeding Towards Work Zones

Computer Vision-based Speeding Monitoring Background

Vehicle speed detection has been investigated using a variety of approaches. In order to estimate traffic speed using digital video recorded with a stationary camera, Rad et al. (2010) suggested a method that involved comparing the vehicle's location between the current frame and the preceding frame. Geometric formulae were used to calibrate the camera. The system created by Rad et al. has the potential to be expanded into additional application areas and has a detected vehicle speed average inaccuracy of 7 km/h. Ferrier et al. (1994) obtained different metrics, including vehicle speed, using real-time tracking approaches by exploiting the motion parameters in the frame and information on the projection between the ground plane and the image plane. They also utilized scene-particular tuning of the flow for a more precise forecast of the target area by the tracker. Yamazaki et al. (2008) utilized digital aerial photos to extract the vehicles and shadows from two successive frames in order to identify vehicle speed. By connecting the respective cars from these photographs based on their proximity, arrangement, and size, as well as by using the distance between the related vehicles and time lag, the speed was determined. The

mapping of coordinates from the picture domain to the real-world domain was also used by Wu et al. (2009). For speed detection, Liu and Yamazaki (2009) employed a pair of panchromatic and multi-spectral QuickBird pictures. In order to estimate speeds, Gerat et al. (2017) combined optical flow methods with Kalman filtering. The former aids in preventing the issue of transient occlusions, while the latter gives more precise speed delivery. Amit Kumar et al. (2018) presented a cutting-edge method for estimating vehicle speed from monocular recordings. Without requiring 3D modeling of structures or vehicles or explicit camera calibration, the suggested method may accurately estimate the speed. To predict vehicle speed, Hua et al. (2018) integrated deep learning models with a traditional computer vision technique. A multi-camera tracking framework was proposed by Tian et al. (2018) based on the combination of visual and semantic highlights. Semantic highlights, counting direction smoothness, speed alteration, and transient data were combined into a bottom-up clustering procedure for information affiliation in each camera view. To monitor the approximate vehicle speed data that are retrieved by the YOLOv3 and the Kalman filter, Liu et al. (2019b) developed a Gaussian filter. In many disciplines, the Kalman filter has shown to be a reliable method for resolving object tracking problems. When objects are successfully recognized, Bochinski et al (2017) demonstrated that simple trackers can be superior to more complicated ones. Kocur and Ftáčnik (2020) proposed a method for identifying the 3D bounding boxes of moving objects, followed by tracking and speed estimation. The system's inaccuracy, nevertheless, still ranges from 30% to 40%. Mejia et al. (2021) proposed a method employing homography and YOLOv4 object detectors that can estimate vehicle speed. Wang (2016) developed a method for detecting moving targets in the video by mapping the relationship between pixel distance and real distance. In this technique, characteristics from moving vehicles were extracted using three-frame differencing and background differences. Then, tracking and positioning were performed utilizing the extraction of vehicle centroid features. While speed detection using computer vision models is not a new research area, its application has not been investigated for detecting speeding events and issuing warning messages to workers at work zones through a smartphone app.

Speed Detection Method

Both parts of the application use the same GUI. Whenever a car approaches the work zone with a higher-than-allowed speed, the framework detects the car and warns workers to leave the area via a specific alarm and the message “A car is approaching the work zone.” This message would be shown on the application user interface and will appear on the server computer as well.

Detecting Speeding Events

A deep learning model was used to classify and detect objects in video frames captured with traffic cameras installed (see Figure 9) at an intersection (H St and Broadway) in the City of Chula Vista. After detecting the object's characteristics—such as bounding box geometry, position, and velocity—in real-time, the data was stored, and then if any object had a velocity higher than a threshold, a warning message was generated and sent to the workers. Figure 10 shows the region of interest at the intersection with a hypothetical work zone considered for the

safety analysis of the work zone. Figure 11 also shows the perspective of the traffic camera used in this study.

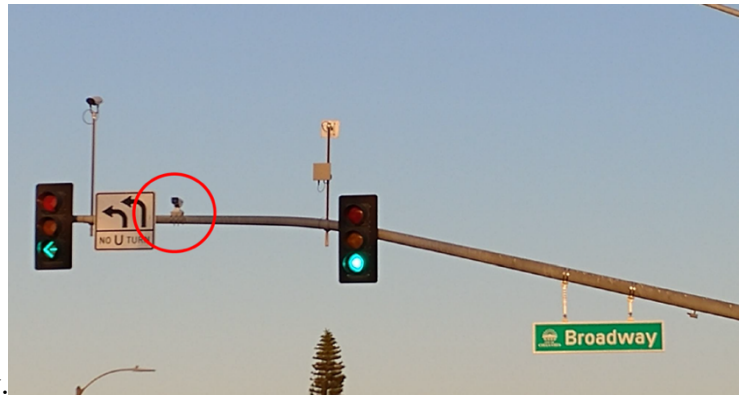

Figure 9. Traffic camera installed on the arm mast of the traffic light at H St and Broadway in the Chula Vista.

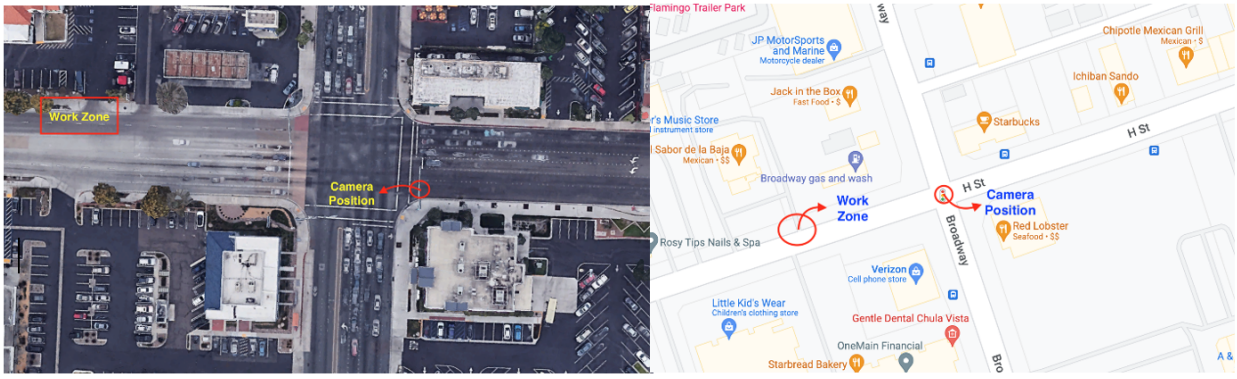

Figure 10. Region of interest showing the hypothetical location of a work zone and traffic camera placement at H St and Broadway in the city of Chula Vista.

Figure 11. The perspective of H St.

Object Detection Models

The availability of relatively affordable computer infrastructure, developments in big data science, and advancements in parallel algorithms have all contributed to the rapid expansion of deep learning research (Shourov et al., 2021). Two tasks are typically solved by object detection models: the first is finding an arbitrary number of objects, and the second is categorizing and calculating the size of a detected object using a perimeter bounding box. All of these tasks are accomplished with computer vision using the OpenCV library in Python. Two types of object detection models—two-stage models and one-stage models—can be distinguished. Examples of two-stage models include RCNN (Bappy et al., 2016), SPPNet (Purkait et al., 2017), Fast RCNN (Girshick. 2015), Faster RCNN (Ren et al., 2015), Mask R-CNN (He et al., 2017), Pyramid Networks (Lin et al., 2017), and G-RCNN (Pramanik et al., 2022). Examples of one-stage models include YOLO (Redmon et al., 2016), SSD (Liu et al., 2016), RetineNet (Li et al., 2020), YOLOv3 (Redmon et al., 2018), YOLOv4 (Bochkovskiy et al., 2020), YOLOR (Wang et al., 2021), and YOLOX (Ge et al., 2021).

One-stage object detectors are a model type that integrates the two tasks into one phase in order to increase performance. In two-stage models, before deep features are used for classification and determining the bounding box, the estimated location of the object regions is proposed using these features. Two-stage detectors are typically more accurate but often require higher computation resources. One-stage detectors take less computing time and are better suited for real-time applications since they forecast the position and dimension of bounding boxes without the region proposal step. In this study, our goal was to issue warning messages in real-time, which directed us to choose a model that performed in real-time.

The YOLO series continually seeks the ideal speed and accuracy trade-off for real-time applications as object detection progresses. The most recent series of YOLO is YOLOX, which is what we used in this study. In comparison to its competitors, YOLOX achieves a superior balance between speed and accuracy across all model sizes. It is noteworthy that YOLOX has improved the YOLOv3 architecture to 47.3% average precision on COCO, beating the industry standard by 3.0% average precision. COCO is a large dataset with 328,000 photos of people and common items which can be used to train machine learning models to label, detect, and describe objects. A wide variety of realistic pictures from the COCO dataset are available, including disorganized scenes with different backgrounds and overlapping objects. A detailed explanation of the YOLOX can be found in Ge et al. (2021).

Speed Detection

In order to determine the speed of the vehicles within the affected intersection, object detection and object tracking are expressed using YOLOX, OpenCV, and Python. A starting line of detection was placed, as shown in Figure 11 (right) where the vehicles exit the intersection. Once vehicles traveling westbound cross this line, their speed is estimated and compared to a threshold. This estimation comprises the following components: storing the first and second center points of a bounding box object, distance in pixels estimation, distance in meters conversion, frames per second to time conversion, and meters per second to mile per hour conversion.

As a vehicle travels through the intersection, a bounding box and its centroid are instantiated and tracked continuously across each frame. Using the camera's pixelated viewing dimensions as a reference coordinate plane, the first frame of vehicle detection stores the horizontal and vertical locations of the vehicle's first centroid. The next frame stores the second horizontal and vertical locations of the vehicle's second centroid. Applying the Pythagorean Theorem, the Euclidean pixel distance that the vehicle traveled is calculated based on the first and second centroid coordinates. This distance in pixels is then converted to meters by measuring the real distance traveled by one base vehicle. The amount of pixels traveled by the vehicle is divided by the real distance traveled, equating to the pixels per meter constant. *It is important to note that the pixels per meter value must be dynamically calibrated further to compensate for the viewing angle of the camera with respect to the plane on which the vehicles travel*. Distance in meters is found by the division of the pixel distance by the pixels per meter value. A frames per second variable value of 30 is assigned based on the specifications of the camera used, which is then inverted to find the variable value for time (1/30 fps). The finalized values of distance and time are respectively represented as numerator and denominator to estimate the speed of the vehicle in meters per second. Finally, meters per second are converted to mile per hour, which is the final estimated speed integer returned.

Speed Detection Results

As mentioned earlier, a vehicle's speed is detected as soon as the vehicle crosses a hypothetical line (see Figure 12). The exact location of this line can be adjusted in order to allow adequate time

for the workers to exit their specified work zone. In that case, the conversion from pixels to meters must be modified. Objects closer to the camera occupy higher pixel counts than objects further away from the camera. In an effort to relay the alert notification to the work zone safety application, modifications to the program must be made to compare the current vehicle speed to an arbitrarily safe constant threshold speed before storing the data in a JSON file. The speed threshold used in this study was the speed limit of 35 mph.

For each object, a specific ID was assigned, and after crossing the desired line, data such as time, center coordinates, speed, and the object's name were recorded to a JSON file in real-time. Also, the same data were stored in a CSV file for debugging and monitoring the program. Appendix B shows an example of data stored in a CSV file for a few objects.

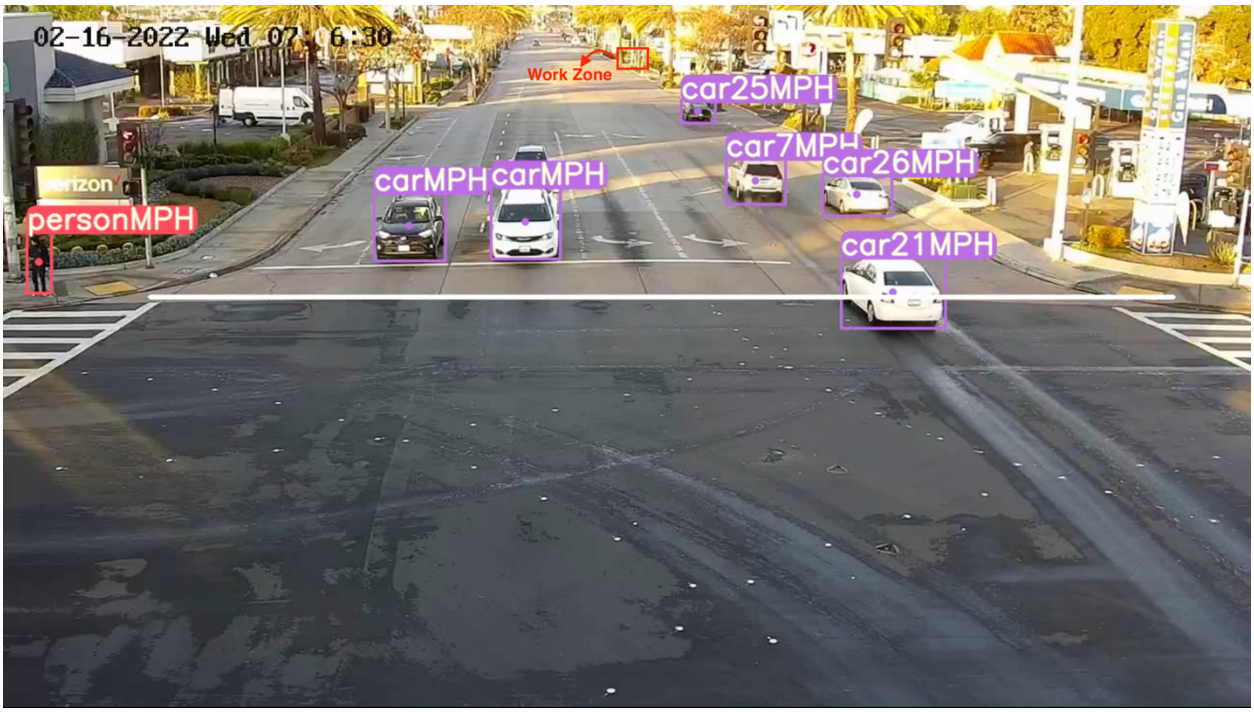

Figure 12. Vehicles' speed detected as they exit the intersection.

Conclusions and Recommendations

This project focuses on two key safety concerns for workers in construction work zones: the health impact of using high vibration power tools such as jackhammers as well as the safety risks of speeding vehicles approaching work zones. Toward this goal, a smartphone application was developed to detect unsafe levels of vibration based on international safety standards. The application leverages embedded sensors in smartphones to estimate the safe amount of time the worker can be exposed to the level of vibration they are experiencing. This number is dynamically updated based on the vibration level and exposure duration. The application also receives an alarm

trigger from connected servers when a speeding vehicle is detected by cameras installed before the work zone.

This project is a first attempt at developing a holistic approach toward internal and external safety of work zone workers, and thus also has some limitations. First, the vibration estimation methodology was tested only on one worker. While this was a proof-of-concept experiment to see if the application alarm goes off at the correct moment, testing on more than one worker doing the exact same activity would help to evaluate the consistency of the developed system in detecting hazards. Second, the experiment was conducted in a single shift at one job site. It is not certain that the range of exposures measured is representative of all activities that cause vibration to the body, even though there is no reason to suspect that results from exposures to other activities not monitored here would be any different. Third, the data was collected by sensors embedded in a smartphone. While this allowed using a lower number of data collection, analysis, and communication gadgets, the frequency limit of 20 Hz compared to a commercial vibration sensor that can record data with a frequency of 4,500 Hz can be a constraint in activities with very high-frequency levels. Fourth, it is possible that the vibration produced by the equipment and that transmitted to the arm (and the wearable sensor) are different due to a damping effect. The research team is exploring this potential effect in a series of different experiments. Fifth, the thresholds for vibration and speed can only be changed in the program's main code, not in the application interface. Sixth, the reliance on surveillance cameras installed in road intersections limits the applicability of the designed speed detection method to urban environments. Finally, the developed framework to alert workers of potential hazards due to speeding vehicles approaching could be further extended to send a message to oncoming drivers to prevent or mitigate potential accidents with workers at work zones.

HAV exposure poses a potential hazard to workers that can be mitigated by the proposed system, despite the limitations listed above. In response to the health hazards posed by HAV exposure, the following recommendations are made. It is important to implement a safety monitoring program, similar to the developed application in this project, designed to detect HAVS early. Breaks from work to avoid HAV exposure should be provided to employees. Rotating employees between jobs that require the use of power hand tools and jobs that do not require them is one way to provide the required break from exposure. Further, the potential hazards and standard of exposure to HAV should be explained to employees. Moreover, employees should be taught to grip vibrating tools as lightly as it is safely possible to do so, thereby minimizing vibration transmitted into their hands.

Additional Products

Education and Workforce Development Products

This project provided partial support for three graduate students in the Department of Civil, Construction and Environmental Engineering as well as the Computational Science Research

Center at SDSU toward their MS Degrees. Graduate student Binh Pham has assisted with initial literature review, vibration standard explorations, and laboratory-scale data collection. Graduate student Farid Shahnavaz has assisted with the majority of the work after the initial phase and developed the smartphone application, conducted real-world data collection, and established the link between vibration standards and developed tools. Graduate student Sina Salehipour has assisted with the development of the computer vision algorithms for speed detection. All students helped with the writing of this report as well as associated journal and conference article drafts.

This research has been presented by Farid Shahnavaz, MS student, at the SDSU Student Research Symposium in 2022.

Furthermore, the PIs designed educational materials on technology-enabled safety in construction and transportation systems. More specifically, Dr. Akhavian developed course modules in *CONE 652: Construction Operations Modeling and Technology* and Dr. Jahangiri developed course modules in *CIVE: 696 Intelligent Transportation Systems*.

Presentation at Explore SDSU, as proposed in the Work Plan was not possible due to the Covid-19 outbreak.

Technology Transfer Products

This findings of this project are reported in a conference paper and a journal paper, both of which to be submitted in the next few months. The conference paper is entitled "A Wearable Safety Alert System for Fieldworkers Exposed to High-Vibration Hand Tools" and will be presented at the 2023 European Council on Computing in Construction (EC3). The Journal paper is entitled "A Holistic Work Zone Safety Alert System through Automated Video and Smartphone Sensor Data Analysis" and will be submitted to the Transportation Research Part C: Emerging Technologies.

The work has been also presented in a number of webinars and meetings including SDSU Research Foundation Board of Directors meeting, SDSU College of Engineering Dean's Advisory Board Meeting, SDSU Department of Civil, Construction, and Environmental Engineering Industry Advisory Board Meeting, Texas A&M Department of Construction Science Graduate Seminar Meeting, and San Diego Lean Construction Institute (LCI) Community of Practice meeting.

The presentation at the Caltrans Annual Statewide Innovation Expo, as proposed in the original Work Plan was cancelled due to the Covid-19 outbreak.

Data Products

Datasets generated as part of this project are available at: https://safed.vtti.vt.edu/projects/a-holistic-work-zone-safety-alert-system-through-automated-video-and-smartphone-sensor-data-analysis/

References

A. G. Rad, A. Dehghani, and M. R. Karim (2010). Vehicle speed detection in video image sequences using cvs method. *International Journal of Physical Sciences, 5*(17):2555-2563.

Aarhus, L., Veiersted, K., Nordby, K., & Bast-Pettersen, R. (2019). Neurosensory component of hand-arm vibration syndrome: a 22-year follow-up study. *Occupational Medicine, 69*(3), 215-218.

Akhavian, R., & Behzadan, A. H. (2016). Smartphone-based construction workers' activity recognition and classification. *Automation in Construction, 71*, 198-209.

Alvarez, P., Bogen, O., & Levine, J. D. (2019). Interleukin 6 decreases nociceptor expression of the potassium channel KV1. 4 in a rat model of hand-arm vibration syndrome. *Pain, 160*(8), 1876.

American National Standards Institute (ANSI). (2006). *Guide For The Measurement And Evaluation Of Human Exposure To Vibration Transmitted To The Hand.* Retrieved from https://webstore.ansi.org/Standards/ASA/ansis2702006.

Armstrong, T. J., Fine, L. J., Radwin, R. G., & Silverstein, B. S. (1987). Ergonomics and the effects of vibration in hand-intensive work. *Scandinavian journal of work, environment & health, 13*(4), 286-289.

Aryal, A., Ghahramani, A., & Becerik-Gerber, B. (2017). Monitoring fatigue in construction workers using physiological measurements. *Automation in Construction, 82*, 154-165.

Bappy, J. H., & Roy-Chowdhury, A. K. (2016). CNN based region proposals for efficient object detection. In *2016 IEEE International Conference on Image Processing (ICIP).*

Baron, J. (2004). Learn From the Safest: Work-Zone Safety Establishes a Stronger Presence in the Classroom. *Roads & Bridges, 42*(1).

Bernard, B., Nelson, N., Estill, C. F., & Fine, L. (1998). The NIOSH review of hand-arm vibration syndrome: vigilance is crucial. *Journal of Occupational and Environmental Medicine, 40*(9), 780-785.

Bochkovskiy, A., Wang, C.-Y., & Liao, H.-Y. M. (2020, April 23). *Yolov4: Optimal Speed and accuracy of object detection. arXiv preprint arXiv:2004.10934.*

Bovenzi, M., Schust, M., & Mauro, M. (2017). An overview of low back pain and occupational exposures to whole-body vibration and mechanical shocks. *Med Lav, 108*(6), 419-433.

Burström, L., Nilsson, T., & Wahlström, J. (2015). Whole-body vibration and the risk of low back pain and sciatica: a systematic review and meta-analysis. *International archives of occupational and environmental health, 88*(4), 403-418.

Castleman, B. I., & Ziem, G. E. (1994). American conference of governmental industrial hygienists: Low threshold of credibility. *American journal of industrial medicine, 26*(1), 133-143.

Cheng, T., Migliaccio, G. C., Teizer, J., & Gatti, U. C. (2013). Data fusion of real-time location sensing and physiological status monitoring for ergonomics analysis of construction workers. *Journal of Computing in Civil engineering, 27*(3), 320-335.

Coggins, M. A., Van Lente, E., Mccallig, M., Paddan, G., & Moore, K. (2010). Evaluation of hand-arm and whole-body vibrations in construction and property management. *Annals of occupational hygiene, 54*(8), 904-914.

Everett, J. G. (1999). Overexertion injuries in construction. *Journal of construction engineering and management, 125*(2), 109-114.

Exposure to Vibration Transmitted to the Hand. In *S2.70: Acoustical Society of America.*

Ferrier, N. J., Rowe, S. M., & Blake, A. (1994, December). Real-time traffic monitoring. In *Proceedings of 1994 IEEE Workshop on Applications of Computer Vision.*

Ge, Z., Liu, S., Wang, F., Li, Z., & Sun, J. (2021, August 6). Y*olox: Exceeding Yolo Series in 2021.*

Girshick, R. (2015). Fast R-CNN. 2015 *IEEE International Conference on Computer Vision (ICCV).*

Griffin, M. (1980). *Vibration injuries of the hand and arm: their occurrence and the evolution of standards and limits.*

Griffin, M. J., & Bovenzi, M. (2002). The diagnosis of disorders caused by hand-transmitted vibration: Southampton Workshop 2000. *International archives of occupational and environmental health, 75*(1), 1-5.

Grinberg, M. (2018). *Flask web development: developing web applications with python.* O'Reilly Media, Inc.

He, K., Gkioxari, G., Dollar, P., & Girshick, R. (2017). Mask R-CNN. *2017 IEEE International Conference on Computer Vision (ICCV).*

Henderson, P., & Ferrari, V. (2017). End-to-end training of object class detectors for mean average precision. Computer Vision. *In Asian Conference on Computer Vision*, 198-213.

Ho, S., & Yu, H. (1989). Ultrastructural changes of the peripheral nerve induced by vibration: an experimental study. *Occupational and Environmental Medicine, 46*(3), 157-164.

De la Hoz-Torres, M. L., Aguilar-Aguilera, A. J., Martínez-Aires, M. D., & Ruiz, D. P. (2019, September). Assessment of whole-body vibration exposure using ISO2631-1: 2008 and

ISO2631-5: 2018 standards. In *INTER-NOISE and NOISE-CON Congress and Conference Proceedings, 259*(5), 4511-4520). Institute of Noise Control Engineering.

International Organization for Standardization (ISO). (1986). *ISO 5349:1986.* Retrieved from https://www.iso.org/standard/11369.html.

International Organization for Standardization (ISO). (1997). *ISO 2631-1:1997.* Retrieved from https://www.iso.org/standard/7612.html.

Jahanbanifar, S., & Akhavian, R. (2018). Evaluation of wearable sensors to quantify construction workers muscle force: An ergonomic analysis. In *2018 Winter Simulation Conference (WSC)* (pp. 3921-3929). IEEE.

Jebelli, H., Hwang, S., & Lee, S. (2018). EEG-based workers' stress recognition at construction sites. *Automation in Construction, 93*, 315-324.

Jeelani, I., Asadi, K., Ramshankar, H., Han, K., & Albert, A. (2021). Real-time vision-based worker localization & hazard detection for construction. *Automation in Construction, 121,* 103448.

Kim, K., & Cho, Y. K. (2021). Automatic recognition of workers' motions in highway construction by using motion sensors and long short-term memory networks. *Journal of construction engineering and management, 147*(3), 04020184.

Langsley, D., Machotka, P., & Flomenhaft, K. (1981). Vibration syndrome again. *British Medical Journal, 282*, 1739.

Li, Y., Dua, A., & Ren, F. (2020). Light-weight RetinaNet for object detection on edge devices. *2020 IEEE 6th World Forum on Internet of Things (WF-IoT).*

Lin, T.-Y., Dollar, P., Girshick, R., He, K., Hariharan, B., & Belongie, S. (2017). Feature Pyramid Networks for Object Detection. *2017 IEEE Conference on Computer Vision and Pattern Recognition (CVPR).*

Liu, W., & Yamazaki, F. (2009). Speed detection of moving vehicles from one scene of QuickBird images. *2009 Joint Urban Remote Sensing Event.*

Liu, W., Anguelov, D., Erhan, D., Szegedy, C., Reed, S., Fu, C.-Y., & Berg, A. C. (2016). *SSD: Single shot multibox detector. Computer Vision - ECCV 2016, 21-37.*

Lundborg, G., Dahlin, L. B., Danielsen, N., Hansson, H. A., Necking, L. E., & Pyykkö, I. (1987). Intraneural edema following exposure to vibration. *Scandinavian Journal of Work, Environment & Health, 13*(4), 326-329.

Miller, R. F., Lohman, W. H., Maldonado, G., & Mandel, J. S. (1994). An epidemiologic study of carpal tunnel syndrome and hand-arm vibration syndrome in relation to vibration exposure. *The Journal of hand surgery, 19*(1), 99-105.

Nnaji, C., Jafarnejad, A., & Gambatese, J. (2020). Effects of wearable light systems on safety of highway construction workers. *Practice Periodical on Structural Design and Construction, 25*(2), 04020003.

Occhipinti, E. (2008). International standards on repetitive actions at high frequency. Research unit. In *Ergonomics of posture and movement.* Don Gnocchi foundation.

Omae, K., Takebayashi, T., & Sakurai, H. (1999). Occupational exposure limits based on biological monitoring: the Japan Society for Occupational Health. *International archives of occupational and environmental health, 72*(4), 271-273.

Pelmear, P. L., & Leong, D. (2000). Review of occupational standards and guidelines for hand-arm (segmental) vibration syndrome (HAVS). *Applied Occupational and Environmental Hygiene, 15*(3), 291-302.

Pramanik, A., Pal, S., Maiti, J., & Mitra, P. (1970, January 1). *Granulated RCNN and multi-class deep sort for multi-object detection and tracking*. Semantic scholar.

Purkait, P., Zhao, C., & Zach, C. (2017, December 9). *SPP-net: Deep absolute pose regression with synthetic views.*

Redmon, J., & Farhadi, A. (2018, April 8). *Yolov3: An incremental improvement.*

Redmon, J., Divvala, S., Girshick, R., & Farhadi, A. (2016). You only look once: Unified, real-time object detection. *2016 IEEE Conference on Computer Vision and Pattern Recognition (CVPR).*

Ren, S., He, K., Girshick, R., & Sun, J. (2017). Faster R-CNN: Towards real-time object detection with region proposal networks. *IEEE Transactions on Pattern Analysis and Machine Intelligence, 39*(6), 1137-1149.

Reynolds, D. D. (2006). Revision Of *ANSI S3. 34 (2.70-2006)-Guide For The Measurement And Evaluation Of Human Exposure To Vibration Transmitted To The Hand-Introduction; Proceedings Of The First American Conference On Human Vibration.*

Rezatofighi, H., Tsoi, N., Gwak, J. Y., Sadeghian, A., Reid, I., & Savarese, S. (2019). Generalized intersection over union: A metric and a loss for bounding box regression. *2019 IEEE/CVF Conference on Computer Vision and Pattern Recognition (CVPR).*

Savage, R., Burke, F., Smith, N., & Hopper, I. (1990). Carpal tunnel syndrome in association with vibration white finger. *The Journal of Hand Surgery: British & European Volume, 15*(1), 100-103.

Shen, S. C., & House, R. A. (2017). Hand-arm vibration syndrome: What family physicians should know. *Canadian Family Physician, 63*(3), 206-210.

Shourov, C. E., Sarkar, M., Jahangiri, A., & Paolini, C. (2021). Deep Learning Architectures for skateboarder-pedestrian surrogate safety measures. *Future Transportation, 1*(2), 387-413.

Takeuchi, T., Takeya, M., & Imanishi, H. (1988). Ultrastructural changes in peripheral nerves of the fingers of three vibration-exposed persons with Raynaud's phenomenon. *Scandinavian Journal of Work, Environment & Health, 14*(1), 31-35.

Wang, C.-Y., Yeh, I.-H., & Liao, H. (1970, January 1). *You only learn one representation: Unified Network for multiple tasks.* Semantic scholar.

Wang, J.-xiang. (2016). Research of vehicle speed detection algorithm in video surveillance. *2016 International Conference on Audio, Language and Image Processing (ICALIP).*

Wijethunga, M., & Ilmini, W. (2020). Air Quality Predicting System for Colombo City using Machine Learning Approaches. *13th International Research Conference, General Sir John Kotelawala Defence University.*

Work Zone Data. *The National Work Zone Safety Information Clearinghouse.* https://workzonesafety.org/work-zone-data/#national. Accessed August 14, 2022.

Wu, J., Liu, Z., Li, J., Gu, C., Si, M., & Tan, F. (2009). An algorithm for automatic vehicle speed detection using video camera. *2009 4th International Conference on Computer Science & Education.*

Yamazaki, F., Liu, W., & Vu, T. T. (2008). Vehicle extraction and speed detection from digital aerial images. *IGARSS 2008 - 2008 IEEE International Geoscience and Remote Sensing Symposium.*

Yang, Z., Yuan, Y., Zhang, M., Zhao, X., & Tian, B. (2019). Assessment of construction workers' labor intensity based on wearable smartphone system. *Journal of Construction Engineering and Management, 145*(7), 04019039.

Zhang, K., Zhao, D., Feng, L., & Cao, L. (2021). Cycling trajectory-based navigation independent of road network data support. *ISPRS International Journal of Geo-Information, 10*(6), 398.

Appendices

Appendix A:

The ISO frequency-weighting factors, W_{hi}, for hand-transmitted vibration for converting magnitudes in one-third octave bands to ISO frequency-weighted magnitudes.

Freq. Band No. (i)	Band Center Freq. (Hz)	Weighting Factor (W_{hi})
6	4	0.375
7	5	0.545
8	6.3	0.727
9	8	0.873
10	10	0.951
11	12.5	0.958
12	16	0.896
13	20	0.782
14	25	0.647
15	31.5	0.519
16	40	0.411
17	50	0.324
18	63	0.256
19	80	0.202
20	100	0.160
21	125	0.127
22	160	0.101
23	200	00799
24	250	0.0634

Freq. Band No. (i)	Band Center Freq. (Hz)	Weighting Factor (W_{hi})
25	315	0.503
26	400	0.398
27	500	0.314
28	630	0.0245
29	800	0.0186
30	1000	0.0135
31	1250	0.00894
32	1600	0.00536
33	2000	0.00295

Appendix B:

An example of data stored in a CSV file for a few objects.

ID	Speed (MPH)	Mode	Centerpoint	Time
ID 19	24	car	(926, 298)	2022_08_15-15h_00m_02s
ID 25	26	truck	(962, 298)	2022_08_15-15h_00m_11s
ID 23	28	car	(1044, 298)	2022_08_15-15h_00m_18s
ID 21	31	car	(1074, 295)	2022_08_15-15h_00m_34s
ID 37	21	car	(912, 296)	2022_08_15-15h_00m_41s
ID 41	27	car	(916, 294)	2022_08_15-15h_00m_48s
ID 17	29	car	(959, 295)	2022_08_15-15h_00m_54s
ID 42	32	car	(933, 297)	2022_08_15-15h_01m_07s
ID 20	46	car	(1069, 299)	2022_08_15-15h_01m_16s
ID 43	35	car	(931, 289)	2022_08_15-15h_01m_27s
ID 51	17	car	(880, 299)	2022_08_15-15h_02m_29s
ID 76	26	car	(1032, 296)	2022_08_15-15h_03m_58s
ID 87	32	car	(940, 299)	2022_08_15-15h_04m_35s
ID 86	29	car	(921, 295)	2022_08_15-15h_04m_36s
ID 88	11	car	(1051, 299)	2022_08_15-15h_05m_05s
ID 89	38	car	(920, 297)	2022_08_15-15h_05m_12s
ID 90	42	car	(1035, 295)	2022_08_15-15h_05m_31s
ID 91	35	truck	(934, 295)	2022_08_15-15h_05m_32s
ID 93	41	car	(927, 296)	2022_08_15-15h_05m_46s
ID 112	12	car	(915, 296)	2022_08_15-15h_06m_21s
ID 135	25	car	(1049, 295)	2022_08_15-15h_07m_34s
ID 134	7	car	(933, 299)	2022_08_15-15h_07m_41s
ID 136	26	car	(1062, 297)	2022_08_15-15h_07m_41s
ID 137	21	car	(912, 295)	2022_08_15-15h_07m_47s
ID 139	36	truck	(938, 288)	2022_08_15-15h_07m_56s
ID 143	38	car	(915, 296)	2022_08_15-15h_08m_03s
ID 142	35	car	(913, 291)	2022_08_15-15h_08m_11s
ID 147	42	car	(914, 291)	2022_08_15-15h_08m_14s
ID 165	28	car	(911, 297)	2022_08_15-15h_09m_28s
ID 173	8	car	(638, 299)	2022_08_15-15h_09m_51s
ID 174	17	car	(886, 299)	2022_08_15-15h_09m_54s
ID 178	10	car	(662, 299)	2022_08_15-15h_09m_57s
ID 181	17	truck	(882, 297)	2022_08_15-15h_10m_03s
ID 176	6	car	(896, 299)	2022_08_15-15h_10m_09s
ID 238	5	truck	(936, 298)	2022_08_15-15h_12m_55s
ID 236	22	truck	(1051, 296)	2022_08_15-15h_12m_58s
ID 230	18	car	(933, 295)	2022_08_15-15h_13m_08s